# Deriving Surface Reflectance From Visible/Near Infrared and Ultraviolet Satellite Observations Through the Community Radiative Transfer Model

Quanhua Liu, Banghua Yan, Kevin Garrett, Yingtao Ma, Xingming Liang, Jingfeng Huang, Wenhui Wang, and Changyong Cao

***Abstract*—Earth's surface reflectance is an important parameter affecting ultraviolet (UV) and visible (VIS) radiance calculations at the top of the atmosphere because many UV and VIS channels can acquire information about the surface and atmosphere. This article provides the theoretical basis for deriving the surface reflectance from satellite-measured UV and VIS observations at window and lower sounding channels with the help of the community radiative transfer model (CRTM) and collocated atmospheric profiles such as ozone, water vapor, and aerosols. Cirrus cloud may be included in the calculation as long as the observations contain enough reflected radiation from the surface. An explicit equation with three scalar parameters $\alpha$, $\beta$, and $\delta$ is obtained for users to calculate Lambertian surface reflectance from the observation. The expressions for the three parameters are somewhat complicated and computationally expansive. We found a simple and smart way that can exactly calculate the three parameters with quasi-linear functions. Numerical experiments using the CRTM simulations have demonstrated the algorithm accuracy for the surface reflectance retrieval better than 2.0E-14. As a case study, measured surface reflectance and the derived surface reflectance over desert from satellite UV measurements are compared. The derived surface reflectance from Suomi National Polar-orbiting Partnership. Visible Infrared Imaging Radiometer Suite (VIIRS) observations and the VIIRS reflectance product are compared as well. In addition, this methodology can also be used to calculate microwave and infrared surface emissivity with scatterings and solar radiation by adding the surface Planck radiance at the surface temperature.**

***Index Terms*—Community radiative transfer model (CRTM), ozone mapping and profiler suites (OMPS) observations and visible infrared imaging radiometer suite (VIIRS) observations, surface reflectance.**

Manuscript received November 15, 2021; revised December 29, 2021; accepted January 30, 2022. Date of publication February 8, 2022; date of current version March 2, 2022. This work was supported by the National Oceanic and Atmospheric Administration (NOAA) Joint Polar Satellite System (JPSS) Proving Ground and Risk Reduction Program (PGRR). *(Corresponding author: Quanhua Liu.)*

Quanhua Liu, Banghua Yan, Kevin Garrett, and Changyong Cao are with the NOAA Center for Satellite Applications and Research, National Environmental Satellite, Data and Information Service, College Park, MD 20740 USA (e-mail: quanhua.liu@noaa.gov; banghua.yan@noaa.gov; kevin.garrett@noaa.gov; changyong.cao@noaa.gov).

Yingtao Ma, Xingming Liang, and Wenhui Wang are with the Cooperative Institute for Satellite and Earth System Studies, Earth System Science Interdisciplinary Center, University of Maryland, College Park, MD 20742 USA (e-mail: yingtao.ma@noaa.gov; xingming.liang@noaa.gov; wenhui.wang@noaa.gov).

Jingfeng Huang is with the Global Science Technologies Inc., Greenbelt, MD 20770 USA, and also with Science Systems and Applications Inc., Lanham, MD 20706 USA (e-mail: jingfeng.huang@noaa.gov).

Digital Object Identifier 10.1109/JSTARS.2022.3149767

## I. Introduction

EARTH'S surface reflectance is an important parameter affecting most of the ultraviolet (UV) and visible (VIS) and near-infrared (NIR) radiance calculations at the top of the atmosphere (TOA), thus, playing a critical role in the calibration/validation of the ozone mapping and profiler suites (OMPS), sensor data record (SDR) [1], [2] ,and Visible Infrared Imaging Radiometer Suite (VIIRS) [3]. The surface reflectance is also a key parameter [4] for the retrieval of aerosols [5], [6], clouds [7], and chemical compositions [8], [9] in the atmosphere from remote sensing data within UV and VIS spectral ranges [10], [11]. Our recent study [12] further showed that the Earth's surface reflectance plays an important role in UV radiance assimilation for total column ozone in the atmosphere. Thus, the information of accurate surface reflectance is highly desirable in UV/VIS satellite data calibration/validation, satellite environmental data record (EDR) retrieval systems, and data assimilation into numerical weather prediction (NWP) models.

Surface reflectance is referred to a spectral reflectance as the ratio between reflected radiance ($I_s$) to downward irradiance ($F_s$) at the surface, that reads as follows [13]:

$$\rho = \frac{\pi I_s}{\mu_0 F_s} \tag{1}$$

where $\mu_0$ is the cosine of a solar zenith angle. Generally speaking, surface reflection has a bidirectional reflectance distribution function (BRDF). However, the Lambertian equivalent reflection, where the surface's reflection is isotropic no matter what downward radiation is, is still a good approximation for many applications [10]. The surface albedo is defined as the fraction of sunlight reflected by the surface of the Earth. The surface albedo is usually a function of solar zenith angles. However, for a Lambertian surface and a given wavelength, the value between the surface albedo and the surface reflectance is the same and the surface emissivity equals one minus the reflectance.

In practice, the surface reflectance may show large variabilities over time and location. Static/climatology surface spectral reflectance library [14]–[16] is very helpful to wide applications. Recently, Tilstra *et al.* [10] generated the Earth's surface reflectivity climatology from UV to NIR observations from Global Ozone Monitoring Experiment (GOME)-2. They retrieve the surface reflectance based on lookup tables, which is very

efficient to process big remote sensing data. The limitations of the technique are that the vertical distribution of absorbing gases, molecular and aerosol scatterings, as well as those interactions cannot be included.

The surface reflectance database is important to climate studies as well and can serve as the first guess in the retrieval. However, the database does not meet the requirement for real-time satellite radiance assimilation and the instrumental radiometric calibration and validation through radiative transfer (RT) calculations. Another approach is to provide surface reflectance available near real-time.[1] However, the product is also based on a lookup table technique. The RT models used for those surface reflectance retrievals are typically not consistent with the radiative transfer model (RTM) used in radiance assimilation and satellite instrumental radiometric calibration. For example, the TOMRAD [17] is used in the satellite ozone and surface effective reflectance product retrieval system (OMPS ATBD, 2014). The inconsistency may be due to different aerosol models, gaseous absorption models, radiative transfer solvers, and other inputs. In direct radiance assimilation, the inputs are from six hours forecast. Those discrepancies call for a need to establish a methodology for surface reflectance calculations using an RTM consistent with that for satellite data calibration and assimilation studies.

In this study, we derive an explicit equation for calculating the surface reflectance from UV VIS and NIR radiances measurements onboard satellites through community radiative transfer model (CRTM). The CRTM has been developed and maintained at the Joint Center for Satellite Data Assimilation (JCSDA) for direct radiance assimilation in support of weather forecast and for operational retrievals of EDRs [18]. In our previous studies [12], we assimilated ozone mapping and profiler suite (OMPS) nadir mapper (NM) radiance [1] for atmospheric column ozone with the information of derived surface reflectance. We used a linear spectral reflectance model that can be determined inline by fitting two OMPS NM channel radiances at 347.6 and 371.8 nm. The two channels have nearly zero sensitivity on atmospheric ozone. Compared with the approach, a new algorithm in this study is established by taking advantages of the CRTM computations.

The rest of this article is organized as follows. The methodology for deriving surface reflectance from satellite measured radiance is described in Section II. Section III discusses the algorithm verification using the CRTM simulations and one case study over Libyan desert site 1 by using OMPS NM measurements and VIIRS measurements. Finally, Section IV concludes this article.

## II. Methodology

For a Lambertian surface, the TOA radiance can be expressed as a sum of cosine and sine harmonic functions [19]–[21] as

$$I\ (\rho,\mu,\phi,\mu_0,\phi_0) = I_0\ (\rho,\mu,\mu_0) + \sum_{m=1}^{M} I_m^c\,(\mu,\mu_0)\cos m\,(\phi_0-\phi) + I_m^s\,(\mu,\mu_0)\sin m\,(\phi_0-\phi)\,. \quad (2)$$

Here, $\mu$ is the cosine of the viewing zenith angle, $\mu_0$ is the cosine of solar zenith angle, $\phi$ is the viewing azimuthal angle, and $\phi_0$ is the solar azimuthal angle. The upper limit $M$ depends on the number of Gaussian quadrature points used for the integration of the radiative transfer equation. One can see from (2) that only the zeroth radiance component depends on the Lambertian surface reflectance. The sine harmonic part is zero for a scalar radiative transfer model. The zeroth radiance component vector at a given wavelength or channel can be obtained in a vector/matrix form as follows [22]:

$$I_0 = S_u\ + T_a(E - r_s R_d)^{-1}\ r_s\left(S_d + V_1\frac{\mu_0 F_0}{\pi}e^{-\frac{\sigma}{\mu_0}}\right). \quad (3)$$

$S_u$ and $S_d$ are the vectors for the diffuse radiation scattered by atmosphere in upward ($u$) and downward ($d$) directions, respectively. $E$ is a unit matrix. $V_1$ is the vector in which all elements equal to one for a scalar radiative transfer. For a fully polarized radiative transfer, each element of $V_1$ is expanded by a transpose of the vector [1,00,0]. To be simple, the derivation below is for a scalar radiative transfer. However, the results are valid for the fully polarized model as well. $T_a$ is the matrix for atmospheric transmission. $R_d$ is the matrix for atmospheric reflection at the bottom of the atmosphere. $\sigma$ is the total optical depth of the atmosphere.

The vectors and matrices in (3) can be evaluated by using Gaussian quadrature points and weights $\mu_i$ and $\mathrm{w_i}$ [23]. In the CRTM, a cosine of the sensor zenith angle $\mu$ is treated as additional quadrature point with zero weight [24]. We use $N$ to represent the number of the quadrature points. The Lambertian surface reflection matrix is defined as

$$r_s\ (\mu_i,\mu_j) = \frac{\rho\mu_j w_j}{\sum_{j=1}^{N}\mu_j w_j}\ . \quad (4)$$

Using (3) and (4), we can obtain the solution of (3) at the sensor zenith angle as (see Appendix A)

$$I_0\ (\rho,\mu,\mu_0) = S_0\ (\mu,\mu_0) + (1-\rho\alpha)^{-1}\rho\,\beta \quad (5)$$

with

$$\beta\ = \frac{t\,(\mu)}{\pi}\ \left(d\,(\mu_0) +\ \mu_0 F_0 e^{-\frac{\sigma}{\mu_0}}\right) \quad (6)$$

where $t(\mu)$ is the diffuse transmission at the sensor observing direction; $\alpha$ and $d(\mu_0)$ are the atmospheric spherical reflectance and downward diffuse flux without the surface reflection at the bottom of the atmosphere, respectively; $S_0(\mu,\mu_0)$ is the upward radiance of the atmosphere.

The actual surface reflectance $\gamma$ can be derived from observed radiance $I^{\mathrm{obs}}$ with the CRTM simulation for an initial nonzero

[1][Online]. Available: https://www.avl.class.noaa.gov/saa/products/welcome;jsessionid = 506D9B420A2144918EDB6EE82A6C5AD8

surface reflectance $\rho$ [see (2) and (5)] as follows:

$$\begin{aligned} I^{\text{obs}}\ (\gamma,\mu,\phi,\mu_0,\phi_0) &= I_0\ (\gamma,\mu,\mu_0) \\ &\quad + \sum_{m=1}^{M} I_m^c\,(\mu,\mu_0)\cos m\,(\phi_0-\phi) \\ &\quad + I_m^s\,(\mu,\mu_0)\sin m\,(\phi_0-\phi) \\ &= I_0\ (\gamma,\mu,\mu_0) + I\,(\rho,\mu,\phi,\mu_0,\phi_0) - I_0\,(\rho,\mu,\mu_0) \\ &= S_0\ (\mu,\mu_0) + (1-\gamma\alpha)^{-1}\gamma\beta + I\,(\rho,\mu,\phi,\mu_0,\phi_0) \\ &\quad - I_0\,(\rho,\mu,\mu_0) \\ &= (1-\gamma\alpha)^{-1}\,\gamma\beta + I\,(\rho,\mu,\phi,\mu_0,\phi_0) + \delta \end{aligned} \tag{7}$$

where

$$\delta\ = S_0\ (\mu,\mu_0) - I_0\,(\rho,\mu,\mu_0)\,. \tag{8}$$

Finally, the surface reflectance corresponding to the observed radiance can be derived from (7) and (8)

$$\gamma\ = \frac{I^{\text{obs}}\,(\gamma,\mu,\phi,\mu_0,\phi_0) - I\,(\rho,\mu,\phi,\mu_0,\phi_0) - \delta}{\beta + \alpha\,(I^{\text{obs}}\,(\gamma,\mu,\phi,\mu_0,\phi_0) - I\,(\rho,\mu,\phi,\mu_0,\phi_0) - \delta)}. \tag{9}$$

One can directly calculate the three scalar parameters $\alpha$, $\beta$, and $\delta$ using their expressions (A6, A9, and A10) in Appendix A. However, the new coding may demand a significant effort and the numerical accuracy ($\sim$0.05%) is not very high because of multiple matrix/vector manipulations including the matrix inversion. Theoretically speaking, one can call the radiative transfer model three times for three surface reflectance values $0,\ \rho,\ \rho_1$, respectively. The three calculated zeroth radiance components can establish three equations [see (5)] for solving the three scalar parameters $\alpha$, $\beta$, and $\delta$. We only call the CRTM one time for the surface reflectance $\rho$ since all layer transmission and reflection matrices, layer source vectors, $I_0(\rho,\mu,\mu_0)$, and $I(\rho,\mu,\phi,\mu_0,\phi_0)$ are computed and saved in single CRTM forward calculation. It is straightforward to write a short subroutine (24 lines code for the algorithm core part) using the saved variables to calculate TOA radiance zeroth component for a given surface reflectance; for example, $I_0(\rho_1,\mu,\mu_0)$ and $I_0(0,\mu,\mu_0)$. We choose $\rho_1 = \frac{\rho}{2}$ . The three results for the three surface reflectances lead to three equations, which are sufficient for calculating the three parameters as follows:

$$\alpha\ = \frac{A\rho - \rho_1}{\rho\rho_1\,(A-1)} \tag{10a}$$

$$\beta\ = \frac{I_0\,(\rho,\mu,\mu_0) - I_0\,(0,\mu,\mu_0)}{\rho}\ (1-\rho\alpha) \tag{10b}$$

$$\delta\ = I_0\ (0,\mu,\mu_0) - I_0\,(\rho,\mu,\mu_0) \tag{10c}$$

where

$$A\ = \frac{I_0\,(\rho_1,\mu,\mu_0) - I_0\,(0,\mu,\mu_0)}{I_0\,(\rho,\mu,\mu_0) - I_0\,(0,\mu,\mu_0)}. \tag{10d}$$

## III. Result and Discussion

In our previous study on OMPS NM radiance assimilation, the surface reflectance of the OMPS NM channels at the wavelengths of 347.6 nm and 371.8 nm are retrieved iteratively [12]. The two channels have nearly zero sensitivity on atmospheric ozone. We interpolated or extrapolated the two reflectance for the reflectance of other OMPS NM channels. We used a finite difference method to calculate the radiance derivative to the surface reflectance by calling the CRTM forward model twice. One can directly calculate Jacobian (same as the derivative) by calling CRTM K-matrix. The Jacobian is also called the sensitivity of radiance to geophysical variables such as aerosol mass and water vapor in the atmosphere. The CRTM Jacobian calculation is very efficient. It takes less than three times of the CRTM forward computational time to calculate Jacobian values for all input variables. In radiance assimilation, the input variables of atmospheric profiles and surface variables are more than hundreds that would demand more than one thousand computational times of the CRTM forward model calculation in a finite difference method. For the surface reflectance retrieval, the finite difference method is fast because it only deals with one variable. It typically takes three iterations to retrieve the surface reflectance and demand computational time about six times of the CRTM forward computation. Contrary to our previous study, the analytic equations in the above section offers users a new approach to calculate surface reflectance from either observations or simulations. It only takes additional 4% CPU time of the CRTM forward model calculation, which is about six times faster than that needed for the traditional retrieval method in [12]. In addition, the analytical algorithm achieves a numerical accuracy while a traditional (iterative) retrieval algorithm achieves an accuracy of about 1%. There is no impact on users who do not need to calculate the surface reflectance. Below, two examples are given to validate the accuracy of the analytical algorithm for deriving the surface reflectance through RTM simulations and satellite observations, respectively.

First, we check the difference between the original surface reflectance and the analytic solution for the surface reflectance through the CRTM. We first call the CRTM by (10a)–(10d) with a constant surface reflectance of 0.4 to compute the three scalar parameters $\alpha$, $\beta$, and $\delta$ for the VIIRS M1 band at 412 nm. In the second step, we simulate the VIIRS M1 band radiance for a set of solar zenith angles and a set of the original surface reflectance: 0.01, 0.1, 0.5, 0.9, 0.99. Finally, we apply (9) and use the simulated VIIRS radiance at the second step as "observation" to retrieve the surface reflectance with $\alpha$, $\beta$, and $\delta$ that are calculated at the first step. The experiments are designed to demonstrate the numerical accuracy of the exactly analytic solution. Table I lists the original and retrieved surface reflectance for a set of the surface reflectance and a set of solar zenith angles. The comparison is limited to the solar zenith angle not larger than 70 degrees because the CRTM model is a plane parallel 1-D radiative transfer model. Spherical coordinate is necessary for very large solar zenith angles. In the simulations, an ECMWF atmospheric profile and a dust mass profile is used. The aerosol optical depth of 0.5 at 550 nm and the effective

TABLE I
COMPARISON BETWEEN ORIGINAL SURFACE REFLECTANCE (VALUES IN THE FIRST ROW) AND DERIVED SURFACE REFLECTANCE FOR THE VIIRS BLUE BAND AT 412 NM FROM THE CRTM SIMULATED RADIANCE OVER LAND

| Surface reflectance<br>Solar zenith angle | 0.01 | 0.1 | 0.5 | 0.9 | 0.99 |
|---|---|---|---|---|---|
| 0 | 0.0100 | 0.1000 | 0.5000 | 0.9000 | 0.9900 |
| 20 | 0.0100 | 0.1000 | 0.5000 | 0.9000 | 0.9900 |
| 40 | 0.0100 | 0.1000 | 0.5000 | 0.9000 | 0.9900 |
| 60 | 0.0100 | 0.1000 | 0.5000 | 0.9000 | 0.9900 |
| 70 | 0.0100 | 0.1000 | 0.5000 | 0.9000 | 0.9900 |

The aerosol Optical depth was set to 0.5 and the corresponding dust effective radius was set to 0.6 $\mu$m. The first guess of the surface reflectance was fixed to 0.4. Equations (10a)–(10d) are used to calculate the parameters $\alpha$, $\beta$, and $\delta$ at the first and then (9) is applied to derive the surface reflectance.

dust radius of 0.6 $\mu$m are chosen. The comparison result shows that the derived surface reflectance agrees well with the true (original) surface reflectance. The maximum difference is less than 2.0E-14, which is a numerical precision. We also test the analytic algorithm by using vectorized CRTM model. The maximum difference is less than 2.0E-14 as well. The analytic solution in (9) and the expressions of $\alpha$, $\beta$, and $\delta$ in (10a)–(10d) are applicable for most radiative transfer models.

The methodology (9) has also been tested with the CRTM simulations for various aerosol optical depths and for different atmospheric profiles. All results showed that the retrieval accuracy of the algorithm achieve the numerical precision, which indicates (9) is strictly an analytic solution for deriving the surface reflectance from radiative transfer simulations.

The second example is the comparison between a measured desert surface reflectance and derived surface reflectance from SNPP OMPS NM and VIIRS observations. The surface measurement [25] is not an *in situ* measurements with the satellite measurements. However, the desert has not been changed. In applications, uncertainties in aerosol optical properties and in observations are very challenging even under clear-sky conditions. Besides, it is difficult to find out *in situ* experiments for the surface reflectance and the associated radiance measurements. Fortunately, we found the measured desert surface reflectance between 297.7 and 400.0 nm [25]. The spectral range covers the OMPS NM UV spectra. We have not found the desert surface reflectance measurement over VIS and NIR spectra. We use the operational VIIRS surface reflectance product [26] for the comparison. The VIIRS surface reflectance product was generated using a lookup table technique based on 6S radiative transfer model [27], [28]. Our comparison is carried out over Libyan desert site 1 on March 2, 2021. The atmospheric and surface parameters were taken from collocated ECMWF analysis. An aerosol mass profile was taken from the Goddard Chemistry Aerosol Radiation and Transport (GOCART) model [29] output. The aerosol mass profile is scaled to fit with the aerosol optical depth at 550 nm given by the VIIRS aerosol product [5], [30]. The VIIRS aerosol optical depth and aerosol particle size product can be downloaded from.[2] Aerosol refractive indices and size

[2][Online]. Available: https://www.avl.class.noaa.gov/saa/products/welcome;jsessionid = D7925CB67FC4E7112F806A32930EB14C

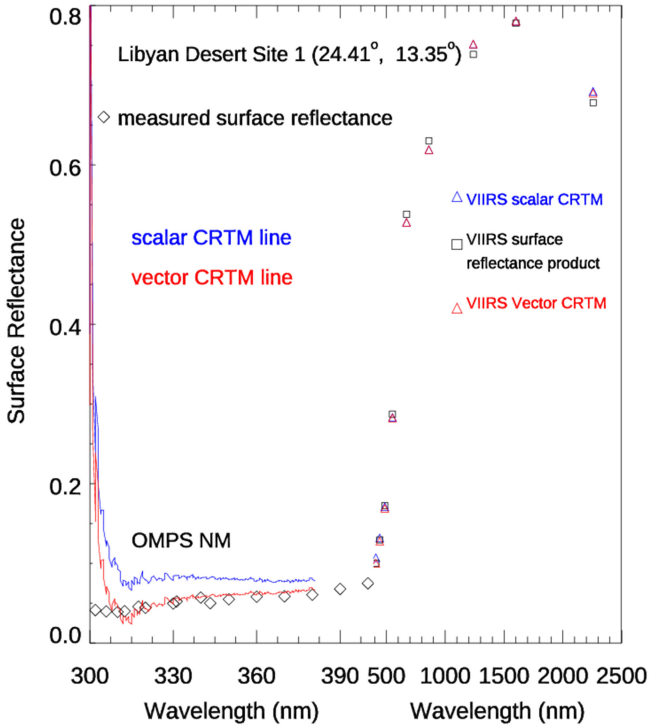


Fig. 1. Comparison between the measured and retrieved surface UV reflectance. The blue line is the retrieved surface reflectance from OMPS NM radiance over Libyan desert site 1. For SNPP VIIRS channels, this retrieved and VIIRS product surface reflectance are compared.

distribution are the most important parts to describe the aerosol optical properties. Laszlo and Liu [30] used a bimodal (fine and coarse) size distribution of spheroidal particles and retrieved VIIRS aerosol optical depth based on a lookup table technique using 6S radiative transfer model [27], [28].

The CRTM uses single size mode of spherical particles. For dust aerosol, different imaginary values of the refractive indices are used in various models. Laszlo [30] accepted the value 0.002 as the imaginary part at the wavelength of 550 nm for the VIIRS aerosol optical depth product. The value is based on the data from AErosol RObotic NETwork (AERONET) sites. The dust refractive imaginary value was 0.005 in the CRTM aerosol optical table. To match with the imaginary value of AERONET [31] at 550 nm, the CRTM imaginary parts of dust refractive indices are multiplied by a factor 0.4 for this study. In this example, the aerosol optical depth was 0.41 and the corresponded dust effective radius was 0.68 $\mu$m according to the collocated VIIRS aerosol optical depth product. As shown in Fig. 1, the UV surface reflectance (red line) is derived from the SNPP OMPS NM measurements by using the vectorized CRTM model. The black diamonds indicate the measured surface desert sand reflectance [25]. The measured and derived surface reflectance agrees well except for the wavelengths between 300 and 310 nm. The measured surface signal between 300 and 310 nm is very weak because of strong ozone absorption and Rayleigh scattering. The path atmospheric transmittance at the wavelength of 300 nm from solar to the surface and to the sensor onboard satellites is less than 1%. Using the scalar CRTM model, the derived

surface reflectance (blue line) is off from the measured surface reflectance.

The red triangles in Fig. 1 represent the derived surface reflectance from the SNPP VIIRS measurements through the vectorized CRTM. The blue triangles in Fig. 1 represent the derived surface reflectance from the SNPP VIIRS measurements through the scalar CRTM. We did not find the measured desert sand surface reflectance for visible band from literatures. The black squares in Fig. 1 are the retrieved surface reflectance that we take from the VIIRS satellite product [26]. For the surface reflectance at blue bands and shortwave infrared bands, our derived surface reflectances agree with the VIIRS satellite product. We found about 2% difference in the surface reflectance for green, red,and NIR bands. The difference is mainly caused by the different aerosol models and radiative transfer models in retrieval algorithms.

There are noticeable differences in derived surface reflectance for OMPS NM ultraviolet channels and the VIIRS blue band between using the scalar and the vectorized CRTM because of strong polarized Rayleigh scattering at short wavelengths. The difference becomes small for VIIRS NIR bands. In general, the vectorized radiative transfer calculations are more accurate, but it demands 16 times more computational resource. It is necessary for the purpose to obtain the accurate surface reflectance. For many applications such as the retrieval of atmospheric ozone and the radiance assimilation for atmospheric ozone, the surface reflectance is an intermediate parameter that is used in radiative transfer calculations. In our previous study [12], we found that the consistency is more important. If we use the scalar CRTM model with the derived surface reflectance from OMPS NM measurements through the scalar CRTM model, the simulated radiance difference against the vectorized CRTM model with the derived surface reflectance through the vectorized CRTM is less than 0.1%. It is worthy to note that the difference between the scalar and vectorized radiative transfer calculations is compensated by the difference between their surface reflectances here.

## IV. Conclusion

This article provides theoretical basis for deriving the surface reflectance and emissivity from satellite-measured radiances through the community radiative transfer model. The algorithm is based on a rigorous radiative transfer model and is simplified for the Lambertian equivalent reflection. Particularly, (9) is obtained for user to calculate the surface reflectance from observations. A simple and smart way [see (10a)–(10d)] is presented to calculate all needed parameters $\alpha$ , $\beta$, and $\delta$. Furthermore, we have demonstrated the accuracy of this methodology through a numerical experiment in Table I. A case study showed that the surface reflectance derived from OMPS NM measurement over Libyan desert site 1 agrees well with a measured surface reflectance. We also derived the OMPS NM and VIIRS surface reflectance for August 9 and September 10, 2021. The derived surface reflectance agreed with the measured desert surface reflectance and the VIIRS surface reflectance product as well. The derived surface UV reflectance is very stable. This implies that the Libyan desert site 1 may be considered as a calibration site for OMPS NM or other UV sensor radiance monitoring and assessment. The surface reflectance derived from SNPP VIIRS observations agrees with VIIRS surface reflectance product in general. Our derived surface reflectance through the CRTM provides important information to future calibration/validation and assimilation developments of OMPS and VIIRS radiance data. In this study, we only discuss UV and VIS surface reflectance. Actually, (5) in this study can also be extended to calculate the infrared and microwave surface emissivity with atmospheric scattering by adding a surface emission term

$$I_0\ (\rho,\mu,\mu_0) = S_0\ (\mu,\mu_0) + (1-\rho\alpha)^{-1}\left[\rho\ \beta + t\,(\mu)\,(1-\rho)\,B\,(T_s)\right] \tag{11}$$

where $B(T_s)$ is the Planck function as a function of the surface temperature $T_s$ and the surface emissivity equals $1-\rho$. The land surface emissivity is the most important parameter to the retrieval of land surface temperature [32]. Therefore, the new methodology with a small change as given in (11) is also applicable for infrared and MW wavelength ranges for surface emissivity estimates in the presence of scatterings and solar radiation.

The surface reflectance under the Lambertian assumption is an effective surface reflectance for giving applications instead of "true" reflectance. Only one measurement at a giving OMPS NM channel is available for us to determine one unknown surface parameter, the effective surface reflectance. For some applications such as the retrieval of atmospheric ozone and the stability monitoring of ultraviolet sensors onboard satellites, we may derive the effective reflectance at the wavelengths insensitive to ozone from the OMPS NM observations in near real time and then interpolate them for the surface reflectance at other wavelengths sensitive to ozone change. The interpolation is a good approximation because the measurements at various wavelengths or channels are for the same surface type and the same sun and sensor viewing directions.

The azimuthal dependence of the surface reflectance can be significant. Generally speaking, the surface reflectance has a BRDF. In order to derive the BRDF that depends on the sun,observation zenith, and azimuthal angles as well as the surface properties, simultaneous measurements for multiple angles are required. The Polarization and Directionality of Earth's Reflectances (POLDER) delivered the data for multiple angles and polarization from 1996 to 2013. Those POLDER data are very valuable for deriving the surface reflectance [33], [34]. The future multiviewing multichannel multipolarisation imager (3MI) is scheduled for launch in 2024.[3]

## Appendix A

To be simple, we derive (5) from (3) using a scalar radiative transfer model. All formulas for the scalar RT are applicable for the vectorized RT. Assuming (it can be any element) the last

[3][Online]. Available: https://www.eumetsat.int/eps-sg-3mi

element of $I_0$ corresponds to the sensor zenith angle ($\mu = \mu_N$)

$$\begin{aligned} I_0(\rho,\mu,\mu_0) = {} & [00,\ldots\ldots,1] \\ & \left(S_u + T_a(E - r_s R_d)^{-1} r_s \left(S_d + V_1 \frac{\mu_0 F_0}{\pi} e^{-\frac{\sigma}{\mu_0}}\right)\right) \\ = {} & S_0(\mu,\mu_0) + [T_a(\mu,\mu_1), T_a(\mu,\mu_2), \ldots\ldots, T_a(\mu,\mu_N)] \\ & \times (E - r_s R_d)^{-1} \frac{\rho}{\pi} \left(d(\mu_0) + \mu_0 F_0 e^{-\frac{\sigma}{\mu_0}}\right) V_1. \end{aligned} \tag{A1}$$

where

$$\begin{aligned} r_s \left(S_d + V_1 \frac{\mu_0 F_0}{\pi} e^{-\frac{\sigma}{\mu_0}}\right) = {} & \sum_{j=1}^{N} \frac{\rho \mu_j w_j}{\sum_{j=1}^{N} \mu_j w_j} S_d(\mu_j) V_1 \\ & + \sum_{j=1}^{N} \frac{\rho \mu_j w_j}{\sum_{j=1}^{N} \mu_j w_j} V_1 \frac{\mu_0 F_0}{\pi} e^{-\frac{\sigma}{\mu_0}} \Bigg) \\ = {} & \frac{\rho}{\pi} \left(d(\mu_0) + \mu_0 F_0 e^{-\frac{\sigma}{\mu_0}}\right) V_1. \end{aligned} \tag{A2}$$

Here

$$d(\mu_0) = \pi \sum_{j=1}^{N} \frac{\mu_j w_j}{\sum_{j=1}^{N} \mu_j w_j} S_d(\mu_j) \tag{A3}$$

is the downwelling diffuse flux. $S_0(\mu,\mu_0)$ and $d(\mu_0)$ include $\mu_0$ because $S_u$ and $S_d$ depend on the cosine of the solar zenith angle. One can also prove

$$(E - r_s R_d)^{-1} V_1 = (1 - \rho\alpha)^{-1} V_1 \tag{A4}$$

which is equivalently to prove

$$(1 - \rho\alpha) V_1 = (E - r_s R_d) V_1. \tag{A5}$$

Comparing the two sides of (A5), one can obtain the atmospheric spheritic reflectance

$$\alpha = \sum_{j=1}^{N} \sum_{i=1}^{N} \frac{\mu_i w_i}{\sum_{j=1}^{N} \mu_j w_j} R_d(\mu_i,\mu_j). \tag{A6}$$

Inserting (A6) into (A1), we will have

$$\begin{aligned} I_0(\rho,\mu,\mu_0) = {} & S_0(\mu,\mu_0) \\ & + [T_a(\mu,\mu_1), T_a(\mu,\mu_2), \ldots\ldots, T_a(\mu,\mu_N)] V_1 \\ & \times (1 - \rho\alpha)^{-1} \frac{\rho}{\pi} \left(d(\mu_0) + \mu_0 F_0 e^{-\frac{\sigma}{\mu_0}}\right) \\ = {} & S_0(\mu,\mu_0) + t(\mu)(1 - \rho\alpha)^{-1} \frac{\rho}{\pi} \left(d(\mu_0) + \mu_0 F_0 e^{-\frac{\sigma}{\mu_0}}\right) \\ = {} & S_0(\mu,\mu_0) + (1 - \rho\alpha)^{-1} \rho\beta. \end{aligned} \tag{A7}$$

Here atmospheric diffuse transmittance

$$t(\mu) = \sum_{j=1}^{N} T_a(\mu,\mu_j) \tag{A8}$$

and

$$\beta = \frac{t(\mu)}{\pi} \left(d(\mu_0) + \mu_0 F_0 e^{-\frac{\sigma}{\mu_0}}\right). \tag{A9}$$

Finally, the zeroth component radiance difference between the surface reflectance 0 and $\rho$ is

$$\delta = S_0(\mu,\mu_0) - I_0(\rho,\mu,\mu_0). \tag{A10}$$

## Appendix B

All equations in the Appendix A are valid for using a fully polarized radiative transfer, except for the index change for the matrices and vectors. For example, (A6) can be expressed as

$$\alpha = \sum_{j=1}^{N} \sum_{i=1}^{N} \frac{\mu_i w_i}{\sum_{j=1}^{N} \mu_j w_j} R_d(\mu_{4\times i-3}, \mu_{4\times j-3}). \tag{B1}$$

A short FORTRAN subroutine for deriving the surface reflectance is included with a CRTM module and plans to be released with the CRTM version 3 in 2022.

## Acknowledgment

The authors would like to thank Dr. H. Liu and Dr. I. Laszlo very much for sharing their great insights on the VIIRS aerosol optical depth product with us. The article contents are solely the opinions of the authors and do not constitute a statement of policy, decision, or position on behalf of NOAA or the U.S. government. The authors thank JPSS PGRR for funding support.

## References

[1] C. Pan *et al.*, "Performance of OMPS nadir profilers' sensor data records," *IEEE Trans. Geosci. Remote Sens.*, vol. 59, no. 8, pp. 6885–6893, Aug. 2021, doi: 10.1109/TGRS.2020.3026586.

[2] L. Flynn *et al.*, "Performance of the Ozone Mapping and Profiler Suite (OMPS) products," *J. Geophys. Res. Atmos.*, vol. 119, pp. 6181–6195, 2014, doi: 10.1002/2013JD020467.

[3] C. Cao *et al.*, "Suomi NPP VIIRS sensor data record verification, validation, and long-term performance monitoring," *J. Geophys. Res. Atmos.*, vol. 118, pp. 11664–11678, 2013, doi: 10.1002/2013JD020418.

[4] S. Liang, *Quantitative Remote Sensing of Land Surfaces*. Hoboken, NJ, USA: Wiley, 2004.

[5] J. M. Jackson *et al.*, "Suomi-NPP VIIRS aerosol algorithms and data products," *J. Geophys. Res. Atmos.*, vol. 118, pp. 12673–112689, 2013, doi: 10.1002/2013JD020449.

[6] H. Liu *et al.*, "Preliminary evaluation of S-NPP VIIRS aerosol optical thickness," *J. Geophys. Res. Atmos.*, vol. 119, pp. 3942–3962, 2014, doi: 10.1002/2013JD020360.

[7] P. Wang, P. Stammes, A. R. van der A, G. Pinardi, and M. van Roozendael, "FRESCO+: An improved O2 A-band cloud retrieval algorithm for tropospheric trace gas retrievals," *Atmos. Chem. Phys.*, vol. 8, no. 21, pp. 6565–6576, 2008, doi: 10.5194/acp-8-6565-2008.

[8] K. F. Boersma *et al.*, "An improved tropospheric NO2 column retrieval algorithm for the ozone monitoring instrument," *Atmos. Meas. Tech.*, vol. 4, no. 9, pp. 1905–1928, 2011, doi: 10.5194/amt-4-1905-2011.

[9] J. Niu, L. Flynn, T. Beck, Z. Zhang, and E. Beach, "Evaluation and improvement of the near-real-time linear fit SO2 retrievals from suomi NPP ozone mapping and profiler suite," *IEEE Trans. Geosci. Remote Sens.*, vol. 59, no. 1, pp. 101–113, Jan. 2021, doi: 10.1109/TGRS.2020.2992429.

[10] L. G. Tilstra, O. N. E. Tuinder, P. Wang, and P. Stammes, "Surface reflectivity climatologies from UV to NIR determined from earth observations by GOME-2 and SCIAMACHY," *J. Geophys. Res. Atmos.*, vol. 122, pp. 4084–4111, 2017, doi: 10.1002/2016JD025940.

[11] L. G. Tilstra, M. de Graaf, I. Aben, and P. Stammes, "In-flight degradation correction of SCIAMACHY UV reflectances and absorbing aerosol index," *J. Geophys. Res.*, vol. 117, 2012, Art. no. D06209, doi: 10.1029/2011JD016957.

[12] Q. Liu, C. Cao, C. Grassotti, X. Liang, and Y. Chen, "Experimental OMPS radiance assimilation through one-dimensional variational analysis for total column ozone in the atmosphere," *Remote Sens.*, vol. 13, 2021, Art. no. 3418. [Online]. Available: https://doi.org/10.3390/rs13173418

[13] S. Chandrasekhar, *Radiative Transfer*. Mineola, NY, USA: Dover, 1960.

[14] J. R. Herman and E. A. Celarier, "Earth surface reflectivity climatology at 340–380 nm from TOMS data," *J. Geophys. Res.*, vol. 102, no. D23, pp. 28003–28011, 1997, doi: 10.1029/97JD02074.
[15] Q. L. Kleipool, M. R. Dobber, J. F. de Haan, and P. F. Levelt, "Earth surface reflectance climatology from 3 years of OMI data," *J. Geophys. Res.*, vol. 113, 2008, Art. no. D18308, doi: 10.1029/2008JD010290.
[16] R. B. A. Koelemeijer, J. F. de Haan, and P. Stammes, "A database of spectral surface reflectivity in the range 335–772 nm derived from 5.5 years of GOME observations," *J. Geophys. Res.*, vol. 108, no. D2, 2003, Art. no. 4070, doi: 10.1029/2002JD002429.
[17] F. Eck, P. K. Bhartia, and J. B. Kerr, "Satellite estimation of spectral UVB irradiance using TOMS derived total ozone and UV reflectivity," *Geophys. Res. Lett.*, vol. 22, pp. 611–614, 1995, doi: 10.1029/95GL00111.
[18] Y. K. Lee, Z. Li, J. Li, and T. J. Schmit, "Evaluation of the GOES-R ABI LAP retrieval algorithm using the GOES-13Sounder," *J. Atmos. Ocean. Technol.*, vol. 31, no. 1, 2014, Art. no. 3019.
[19] R. J. D. Spurr, "VLIDORT: A linearized pseudo-spherical vector discrete ordinate radiative transfer code for forward model and retrieval studies in multilayer multiple scattering media," *J. Quant. Spectrosc. Radiat. Transfer*, vol. 102, pp. 316–342, 2006, doi: 10.1016/j/jqsrt.2006.05.005.
[20] J. Lenoble, *Radiative Transfer in Scattering and Absorbing Atmospheres: Standard Computational Procedures*. Hampton, VA, USA: Deepak Publishing, 1985.
[21] Q. Liu and C. Cao, "Analytic expressions of the transmission, reflection, and source function for the community radiative transfer model," *J. Q. Spectrosc. Radiative Transfer.*, vol. 226, pp. 115–126, 2019. [Online]. Available: https://doi.org/10.1016/j.jqsrt.2019.01.019
[22] Q. Liu and E. Ruprecht, "Radiative transfer model: Matrix operator method," *Appl. Opt.*, vol. 35, pp. 4229–4237, 1996. [Online]. Available: https://www.osapublishing.org/ao/abstract.cfm?URI=ao-35-21-4229
[23] K. Stamnes, S.-C. Tsay, W. Wiscombe, and K. Jayaweera, "Numerically stable algorithm for discrete ordinate method radiative transfer in multiple scattering and emitting layered media," *Appl. Opt.*, vol. 27, pp. 2502–2509, 1988.
[24] K. F. Evans and G. L. Stephens, "A new polarized atmospheric radiative transfer model," *J. Quantitative Spectrosc. Radiative Transfer*, vol. 46, pp. 413–423, 1991.
[25] D. Doda and A. Green, "Surface reflectance measurements in the ultraviolet from an airborne platform, part 2," *Appl. Opt.*, vol. 20, pp. 636–642, 1981.
[26] E. Vermote, E. C. O. Justice, and I. A. Csiszar, "Early evaluation of the VIIRS calibration, cloud mask and surface reflectance earth data records," *Remote Sens. Environ.*, vol. 148, pp. 134–145, 2014, doi: 10.1016/j.rse.2014.03.028.
[27] S. Y. Kotchenova and E. F. Vermote, "Validation of a vector version of the 6S radiative transfer code for atmospheric correction of satellite data. Part II. Homogeneous lambertian and anisotropic surfaces," *Appl. Opt.*, vol. 46, pp. 4455–4464, 2007, doi: 10.1364/ao.46.004455.
[28] S. Y. Kotchenova, and E. F. Vermote, R. Matarrese, and F. J. Klemm, "Validation of a vector version of the 6S radiative transfer code for atmospheric correction of satellite data. Part I: Path radiance," *Appl. Opt.*, vol. 45, pp. 6762–6774, 2006, doi: 10.1364/ao.45.006762.
[29] M. Chin *et al.*, "Tropospheric aerosol optical thickness from the GOCART model and comparisons with satellite and sunphotometer measurements," *J. Atmos. Sci.*, vol. 59, pp. 461–483, 2002.
[30] I. Laszlo, "Remote Sensing of Tropospheric Aerosol Optical Depth From Multispectral Monodirectional Space-Based Observations," in *Comprehensive Remote Sens.*, pp. 137–196, 2018, doi: 10.1016/B978-0-12-409548-9.10389-6.
[31] O. Dubovik *et al.*, "Variability of absorption and optical properties of key aerosol types observed in worldwide locations," *J. Atmos. Sci.*, vol. 59, pp. 590–608, 2002.
[32] Y. Liu, Y. Yu, P. Yu, F. Göttsche, and L. Trigo, "Quality assessment of S-NPP VIIRS land surface temperature product," *Remote Sens.*, vol. 7, pp. 12215–12241, 2015, doi: 10.3390/rs70912215.
[33] P. Lallart, R. Kahn, and D. Tanre, "POLDER2/ADEOSII, MISR, and MODIS/Terra reflectance comparisons," *J. Geophys. Res.- Atmos.*, vol. 113, 2008, Art. no. D14s02, doi: 10.1029/2007jd009656.
[34] F. Nadal and F. M. Breon, "Parameterization of surface polarized reflectance derived from POLDER spaceborne measurements," *IEEE Trans. Geosci. Remote*, vol. 37, no. 3, pp. 1709–1718, May 1999, doi: 10.1109/36.763292.

**Quanhua Liu** received the B.S. degree from the Nanjing University of Information Science and Technology (former Nanjing Institute of Meteorology), Nanjing, China, in 1982, the master's degree in physics from the Chinese Academy of Sciences, Beijing, China, in 1984, and the Ph.D. degree in meteorology and remote sensing from the University of Kiel, Kiel, Germany, in 1992.

He is currently a Physical Scientist with the NOAA/NESDIS Center for Satellite Applications and Research. He is leading NOAA ATMS sensor data record (SDR) calibration and NOAA Microwave Integrated Retrieval System (MiRS) that retrieves ten environmental data records (EDRs). He was a Senior Research Scientist with the University of Maryland, College Park, MD, USA, working as a Co-Chair of the Community Radiative Transfer Model. His research interests include radiative transfer models, satellite products, and sensor calibration and climate studies.

**Banghua Yan** received the Ph.D. degree in atmospheric physics from the Institute of Atmospheric Physics, Chinese Academy of Sciences, Beijing, China, in 1997, and the Ph.D. degree in atmospheric radiation from the University of Alaska, Fairbanks, AK, USA, in 2001.

She is currently a Physical Scientist with the Satellite Calibration and Data Assimilation Branch, NOAA Center for Satellite Applications and Research (STAR). From November 1999 to July 2010, she worked for the STAR through companies or NOAA Joint Center for Satellite Data Assimilation (JCSDA) or the Earth System Science Interdisciplinary Center, University of Maryland, College Park, MD, USA. During this period, she significantly contributed to the developments of microwave land, snow, and sea ice emissivity models, and microwave satellite instrument data assimilation studies. These developments have significantly improved the use of satellite sounding data in numerical weather prediction (NWP) models. The land, snow, and sea ice microwave emissivity models have been implemented into the NOAA NCEP NWP model and the JCSDA community radiative transfer model that has been successfully used in several operational data assimilation systems in the U.S. From August 2010 to August 2017, she was an Oceanographer with the NOAA Office of Satellite Data Processing and Distribution, Camp Springs, MD, USA, to lead the NOAA operational ocean color production system. She has authored or coauthored more than 30 papers in international peer-reviewed journals. In addition, from September 2017 to September 2019, she successfully led calibrations/validations of Metop-C Advanced Microwave Sounding Unit-A (AMSU-A) to ensure the operation of AMSU-A data. She also coordinated the JPSS/STAR (JSTAR) mission program for more than half a year. Currently, she leads calibrations/validations of Joint Polar Satellite System Ozone Mapping and Profiler Suite (OMPS) and the STAR Integrated Calibration/Validation System (ICVS) Long-term Monitoring.

**Kevin Garrett** received the M.S. degree in atmospheric sciences from Texas A&M University, College Station, TX, USA, in 2007.

He is currently a Physical Scientist with the NOAA/NESDIS Center for Satellite Applications and Research (STAR), College Park, MD, USA, and is the Federal Manager with the Community Radiative Transfer Model (CRTM). Additionally, he serves as NESDIS representative to the U.S. Joint Center for Satellite Data Assimilation (JCSDA) Executive Team. Previously, he was a Contractor Task Lead on the NOAA Microwave Integrated Retrieval System (MiRS), supported the JCSDA, leading the optimization of SNPP ATMS and DMSP SSMI/S data assimilation, and implementation of new passive microwave satellite data including GPM GMI, GCOM-W1 AMSR2, and Megha-Tropiques SAPHIR into the NOAA Global Data Assimilation System/Global Forecast System (GDAS/GFS). His research interests include all-sky radiative transfer and applications in passive microwave remote sensing, data fusion, and data assimilation.

**Yingtao Ma** received his Ph.D. degree from the University of Maryland at College Park (UMCP) in 2004, and worked in the Department of Atmospheric & Oceanic Science until 2014, engaged in research on surface radiation budget retrieval and satellite remote sensing. He is a research scientist with the Cooperative Institute for Research in the Atmosphere (CIRA), Colorado State University, Fort Collins. He currently works with the Community Radiative Transfer Model (CRTM) team at NOAA/NESDIS Center for Satellite Applications and Research (STAR), College Park, MD. From 2014- 2018 he worked as a staff scientist for Atmospheric and Environmental Research, Inc. (AER), working on the redesign and enhancement of AER's Line-By-Line Radiative Transfer Model (LBLRTM).

His research interests are atmospheric radiative transfer, remote sensing of the earths atmosphere and surface, surface radiation budget and atmospheric measurements and instrumentation.

**Xingming Liang** received the B.S. degree in construction machinery from Jilin University, Changchun, China, in 1992, and the Ph.D. degree in remote sensing and atmospheric sciences from Saga University, Saga, Japan, in 2005.

He is currently an Assistant Research Scientist with the Cooperative Institute for Satellite Earth System Studies (CISESS), University of Maryland, College Park, MD, USA, and works with the Center for Satellite Applications and Research (STAR) of NOAA/NESDIS on developing Artificial intelligence applications in remote sensing and supporting the development of the Microwave Integrated Retrieval System (MiRS) and the community radiative transfer model (CRTM). From 2007 to 2016, he was a Research Scientist with the Cooperative Institute for Research in the Atmosphere, Colorado State University, Fort Collins, CO, USA. From 2016 to 2019, he was a Senior Scientist with Earth Resources Technology Inc., Silver Spring, MD, USA, and Global Science and Technology Inc., Greenbelt, MD, USA.

**Jingfeng Huang** received the bachelor's degree in 2000 from Tsinghua University, Beijing, China, the master's degree in 2002 from the Hong Kong University of Science and Technology, Clear Water Bay, Hong Kong, and the Ph.D. degree of Civil and Environmental Engineering in 2006 from the University of Manchester, Manchester, England, U.K.

He is currently a Senior Scientist with Science Systems and Applications, Inc. (SSAI), Lanham, MD, USA, and a team member in the NOAA STAR's Integrated Calibration Validation System (ICVS) Team and the OMPS Sensor Data Record (SDR) Team. He works actively on the near real time and long-term monitoring of the multiple sensor instrument stability and SDR data quality. He also works on the intensive OMPS SDR calibration and validation, particularly using radiative transfer models for intersensor cross calibration. With both education and research activities, he has 20 years of experience in environmental science, atmosphere science, and satellite remote sensing, including but not limited to satellite algorithm development, satellite product validation, atmosphere remote sensing, aerosol–cloud–precipitation–climate interactions, radiative transfer model simulations, etc.

**Wenhui Wang** received the B.S. and M.S. degrees in computer science from Xi'an Jiaotong University, Xi'an, China, in 1991 and 1994, respectively, and the Ph.D. degree in geography, specializing in remote sensing from the University of Maryland, College Park, MD, USA, in 2008.

She is currently a Visiting Associate Research Scientist with the Cooperative Institute for Satellite Earth System Studies (CISESS),University of Maryland. From 2018 to 2019, she was a Senior Scientist with the Global Science and Technology, Inc., Greenbelt, MD, USA. From 2013 to 2018, she was a Senior Scientist with the Earth Resources Technology Inc., Silver Spring, MD, USA. From 2008 to 2013, she was a Support Scientist with I. M. Systems Group Inc., Rockville, MD, USA. From 1994 to 2001, she was a Senior Software Engineer with the Institute of Computing Technology, Chinese Academy of Sciences, Beijing, China. Her research interests include satellite instrument calibration and validation, climate data records, surface radiation budget, and geovisualization.

**Changyong Cao** received the B.S. degree in geography from Peking University, Beijing, China, in 1982, and the Ph.D. degree in geography,specializing in remote sensing and geographic information systems from Louisiana State University, Baton Rouge, LA, USA, in 1992.

He is currently a Supervisory Research Physical Scientist and Chief for the Satellite Calibration and Data Assimilation Branch with the NOAA Center for Satellite Applications and Research (STAR/SMCD). He specializes in the calibration of radiometers onboard NOAA's Operational Environmental Satellites, and currently leads the STAR radiance science, as well as the VIIRS sensor science teams. He is well known for his work on intersatellite calibration using the Simultaneous Nadir Overpass (SNO) method, which has become one of the cornerstones for the World Meteorological Organization Global Space-based Inter-Calibration System (WMO/GSICS). He was also former chair of the Committee on Earth Observation Satellites/Working Group on Calibration/Validation (CEOS/WGCV). Before joining NOAA, he was a Senior Scientist with five years of industry experience with a major aerospace company supporting NASA projects.

Dr. Cao was the recipient of three gold, one silver, and several bronze medals honored by the U.S. Department of Commerce and NOAA for the scientific and professional achievements.